Thymosin β_{10} mRNA expression during early postimplantation mouse development

Pablo Carpintero[a], Francisco Franco del Amo[a], Ramón Anadón[b], Jaime Gómez-Márquez[a,*]

[a] *Departamento de Bioquímica y Biología Molecular, Facultad de Biología, Universidad de Santiago, Santiago de Compostela, Spain*
[b] *Departamento de Biología Fundamental, Facultad de Biología, Universidad de Santiago, Santiago de Compostela, Spain*

Received 7 June 1996; revised version received 29 June 1996

Abstract The β-thymosins are a family of monomeric actin sequestering peptides that regulate actin dynamics within the cells. During embryogenesis the control of actin polymerization is essential in processes such as cell migration, angiogenesis and neurogenesis. Here we report that the levels of thymosin β_{10} ($T\beta_{10}$) mRNA strongly increase during early postimplantation mouse embryogenesis as well as during in vitro P19 cell differentiation, indicating that this peptide plays an important role in early development. Moreover, analysis of the spatial distribution of $T\beta_{10}$ mRNA in 9.5–12.5 days postcoitum mouse embryos showed a remarkable presence of this transcript in mesenchymal structures as well as in the mantle layer of spinal cord. Interestingly, we observed differences in the distribution of the mRNAs encoding $T\beta_{10}$ and $T\beta_4$, another member of the β-thymosin family, suggesting different roles for these peptides during mouse embryogenesis.

Key words: Thymosin β_{10}; Actin-binding peptide; P19 cell; Mouse embryogenesis

1. Introduction

The β-thymosins are a family of highly conserved small proteins involved in the control of actin polymerization [1,2]. Thymosin β_4 ($T\beta_4$), a 43 residue peptide, is the most abundant member of this family and it is present in all mammalian species accompanied by its structural homologue thymosin β_{10} ($T\beta_{10}$) in many cell types [3,4]. Although $T\beta_4$ and $T\beta_{10}$ coexist in many tissues at varying ratios, the biological meaning of this association has still to be elucidated. These peptides sequester actin monomers and thereby induce depolymerization of the intracellular F-actin networks [5,6]. They bind to G-actin in a 1:1 complex forming a large pool of unpolymerized actin that can be easily released when needed for the polymerization of actin filaments.

Both β-thymosins are differentially regulated during development [7,8]. Thus, the analysis of steady-state mRNA and protein levels showed that both $T\beta_4$ and $T\beta_{10}$ genes are regulated in the developing rat and human central nervous system [7,9,10]. The $T\beta_{10}$ mRNA was found to be highly expressed in the early phases of human nervous system development but its amount descents to basal levels in the adult brain [9–11] and it has been proposed that cAMP dependent and retinoic responsive mechanisms coordinate $T\beta_{10}$ gene expression during neuroembryogenesis [12]. In contrast, the $T\beta_4$ gene is strongly activated during early phases of neuroembryogenesis [13] and also in the mature brain [7,9,14]. We have previously shown that $T\beta_4$ mRNA is very abundant in different embryonic tissues, principally nerve structures [13] and cardiovascular tissues [15], suggesting that this peptide plays an important role in the development of mouse nervous system as well as in angiogenesis. However, little is known about the expression of the $T\beta_{10}$ gene during early postimplantation mouse development.

In the present work we studied the levels of $T\beta_{10}$ mRNA in culture systems that can undergo cell differentiation. For this purpose we employed the murine P19 embryonal carcinoma cell line, a well-established model for studying cell differentiation as it relates to the early stages of embryogenesis [16]. We also analyzed the spatial and temporal distribution of $T\beta_{10}$ mRNA during early mouse development. We show that the $T\beta_{10}$ gene is expressed early during development mostly in mesenchymal structures and in some areas of the nervous system.

2. Materials and methods

2.1. RNA preparation, ribonuclease protection analysis and in vitro transcription

Postimplantation mouse embryos were recovered at the appropriate stages, considering the day of the vaginal plug as day 0.5 of development. Total RNA was isolated by the acid guanidium thiocyanate-phenol-chloroform technique [17]. Ribonuclease protection assay (RPA) was performed with the RPA II kit (Ambion), following manufacturers' instructions using the α-^{32}P-labelled antisense RNA obtained by in vitro transcription. For the RPA analysis, $T\beta_{10}$ cDNA, kindly provided by Dr. A.K. Hall, was cut with *Avr*II and *Eco*RI, subcloned in the *Xba*I and *Eco*RI site of pGEM3Z (Promega), linearized with *Eco*RI and transcribed using SP6 RNA polymerase, [α-^{32}P]UTP (3000 Ci/mmol, Amersham) and an in vitro transcription kit (Promega). For in situ hybridization, we used a riboprobe derived from the 3′ non-coding region to avoid any cross-hybridization with the homologous $T\beta_4$. Briefly, $T\beta_{10}$ cDNA insert cloned into pBluescript (Stratagene) was digested with *Avr*II and *Hae*III, the 135 bp fragment subcloned in the *Xba*I/*Hin*cII sites of pGEM3Z (pGEM3Z-β_{10}). After linearization with *Eco*RI, transcription was performed with SP6 RNA polymerase using [α-^{33}P]UTP (1000–3000 Ci/mmol, Amersham) as indicated above. As a control of the in situ hybridization experiments, we used the sense probe obtained by in vitro transcription of pGEM3Z-β_{10} with T7 RNA polymerase.

2.2. Cell culture

P19 embryonal carcinoma cells were cultured and differentiated as described elsewhere [16]. Cells were grown in αMEM plus 10% fetal bovine serum. To induce differentiation, cells were placed in suspension culture in agarose-coated dishes either as a single cell suspension or as lightly trypsinized aggregates. Cells in suspension culture were placed either in αMEM plus 10% fetal bovine serum (untreated control) or in the same medium with 0.3 μM retinoic acid (RA) or in the same media in the presence of 0.5% dimethyl sulfoxide (DMSO). After 4 days in suspension, all samples contained aggregates of P19 cells. The differentiation was confirmed by microscopic examination

*Corresponding author. Fax: (34) (81) 596904.
E-mail: bnjgm@usc.es

Abbreviations: $T\beta_4$, thymosin β_4; $T\beta_{10}$, thymosin β_{10}; dpc, days postcoitum; RPA, ribonuclease protection assay; RA, retinoic acid; DMSO, dimethyl sulfoxide

PII S0014-5793(96)00888-5

of cultures. RNA was harvested from these cells and assayed for $T\beta_{10}$ mRNA by RPA using the β-actin mRNA for comparison.

2.3. In situ hybridization

C57BL/6 mouse embryos of 9.5, 10.5, 11.5 and 12.5 days postcoitum (dpc) were dissected and fixed at 4°C in 4% paraformaldehyde in phosphate buffered saline (PBS) overnight. The fixed embryos were dehydrated, embedded in paraffin and 6 μm thick sections were cut and floated onto 3-aminopropyltriethoxysilane-coated slides. Slides were dewaxed in xylene, hydrated in an ethanol series and fixed in fresh 4% paraformaldehyde in PBS. Sections were treated with 15 μg/ml proteinase K (dissolved in 50 mM Tris-HCl, 5 mM EDTA, pH 8.0) for 7.5 min, washed in PBS and postfixed in 4% paraformaldehyde in PBS. Sections were then treated with acetic anhydride, washed and dehydrated. [α-^{33}P]UTP labelled antisense and sense RNA probes were prepared as described above. The probe was resuspended at 600 ng/μl in hybridization solution (50% formamide, 0.3 M NaCl, 20 mM Tris-HCl, 5 mM EDTA, pH 8.0, 10% dextran sulfate, 1×Denhardt's solution, 0.5 mg/ml yeast tRNA). After hybridization overnight at 55°C, sections were incubated with RNase A, washed at high stringency (50% formamide, 2×SSC, 10 mM DTT, 65°C) and dehydrated. Slides were dipped in LM-1 emulsion (Amersham), exposed for 10 days, developed with Kodak D19, stained with hematoxylin-eosin and mounted with Permount (Fischer). Photomicrographs were taken on a Zeiss Axioskop or a Nikon Optiphot microscope.

3. Results and discussion

To gain new insights about the role of $T\beta_{10}$ in cell differentiation and early embryogenesis, we first analyzed the variation of $T\beta_{10}$ mRNA during P19 cell differentiation, a well-established model for this type of studies [16]. Cells were placed in culture either as a single cell suspension or as aggregates and induced to differentiate with RA. Under these conditions P19 cells mostly differentiate into neurons and glial cells. Levels of $T\beta_{10}$ transcript, before and after differentiation, were determined by RPA. As shown in Fig. 1 (P19-RA), the amount of $T\beta_{10}$ mRNA increased significantly after RA treatment. In three different RPA assays carried out with other RNAs, we found that this induction was consistently greater if P19 cells were initially placed in suspension cultures as aggregates rather than in single cell suspension. The observed increase in the levels of β-actin mRNA also suggests changes in the expression of actin genes upon RA-induced differentiation of P19 cells. Cell aggregates look like 'embryoid bodies' with an inner core of embryonal cells surrounded by a ring of cells that resembles primitive endoderm [18]. Therefore the $T\beta_{10}$ activation seems to be favored in in vitro systems that mimic a pluricellular structure that undergoes differentiation. When P19 cells were induced with DMSO (becoming mostly muscle cells), $T\beta_{10}$ transcript levels also showed an elevation, although lower than the induction provoked by RA (Fig. 1, P19-DMSO). Similar results were obtained in the expression analysis of $T\beta_4$ gene during P19 cells differentiation with RA and DMSO [15]. We also analyzed the temporal expression of $T\beta_{10}$ mRNA during mouse embryogenesis. $T\beta_{10}$ transcript was present in all postimplantation stages examined (6.5–10.5 dpc). There is a great increase in the amount of $T\beta_{10}$ mRNA in the transition between 6.5 to 7.5 dpc (Fig. 1) coincident with the end of gastrulation, the head process formation and the beginning of organogenesis. Likewise, $T\beta_4$ mRNA becomes very abundant in the same period of mouse embryogenesis [13]. Altogether these results indicate that both β-thymosins are involved in the control of actin polymerization during early embryonic development.

To study the spatial distribution of $T\beta_{10}$ mRNA during mouse embryogenesis, we carried out in situ hybridization in 9.5–12.5 dpc mouse embryos. In the 9.5 dpc embryos, $T\beta_{10}$ is

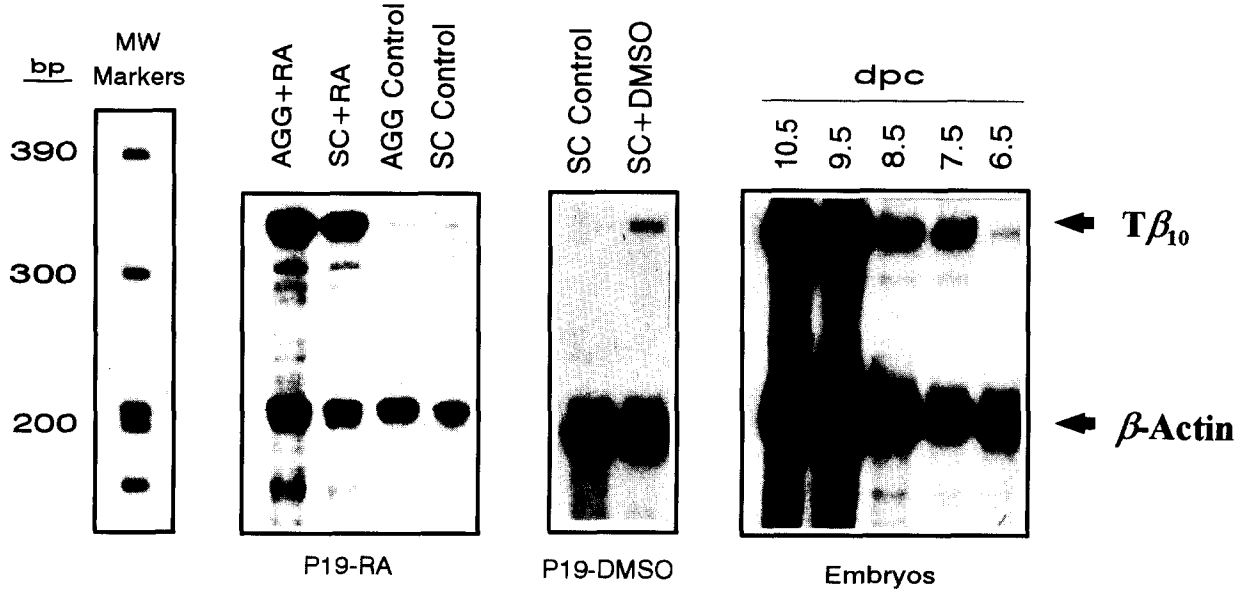

Fig. 1. Analysis of the expression of the $T\beta_{10}$ gene in differentiating P19 embryonal carcinoma cells and during early postimplantation mouse embryogenesis. P19-RA: retinoic acid (RA) induction of $T\beta_{10}$ mRNA in differentiating P19 embryonal carcinoma cells. Total RNA (10 μg) was isolated from single cells (SC), aggregates (AGG), single cells differentiated with 0.3 μM RA (SC+RA) and aggregates differentiated with 0.3 μM RA (AGG+RA), and analyzed by RPA as described in Section 2. SC control and AGG control represent P19 cells untreated with RA. P19-DMSO: induction of $T\beta_{10}$ mRNA during P19 cell differentiation with dimethyl sulfoxide (DMSO). SC control represents P19 cells incubated without DMSO and SC+DMSO are P19 cells differentiated with DMSO. Embryos: $T\beta_{10}$ mRNA expression in postimplantation mouse embryos. Total RNA was isolated from embryos at the indicated days of gestation (dpc) and analyzed by RPA. RNA concentration and integrity was checked by ethidium bromide staining (not shown) and by RPA using the β-actin probe. The data shown here are a representative sample of an experiment repeated three times with independent RNAs.

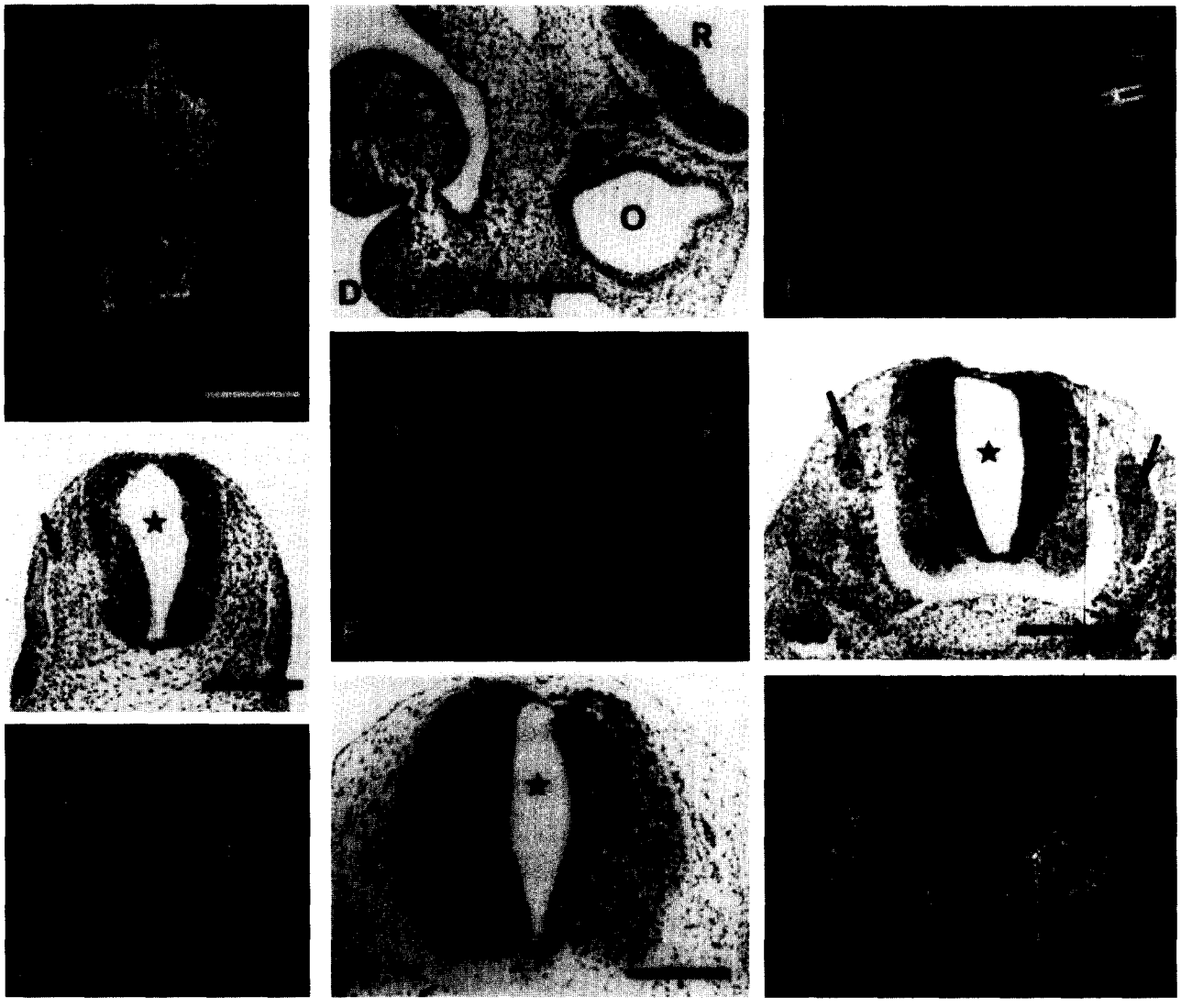

Fig. 2. In situ hybridization of $T\beta_{10}$ probe in mouse embryos. A: Sagittal section of a 9.5 dpc embryo showing high $T\beta_{10}$ expression in mesenchyme (asterisk). Note the low expression in the spinal cord (star) and otocyst (arrow). Wide arrow, mandibular process; H, heart; MN, mesonephros. B, C: Bright and dark field photomicrographs of a transverse section through the cervical region showing the low levels of $T\beta_{10}$ mRNA in the spinal cord neuroepithelium (asterisk) and high expression in the skeletal mesenchyme (arrow). Star, central canal. D, E: Bright and dark field photomicrographs of a sagittal section through the head of a 10.5 dpc embryo showing that $T\beta_{10}$ is mainly expressed in the mesenchyme. Note also low to moderate expression in a cranial (vestibular) ganglion (arrow) and higher expression in the mantle layer of the neural tube which is now appearing (double arrow). MP, mandibular process; O, otocyst; R, rhombencephalon. F, G: Dark and bright field photomicrographs of a transverse section through the trunk region of a 12.5 dpc embryo showing high expression of $T\beta_{10}$ in the mantle layer (M) of the spinal cord. Note the very low level of expression in the neuroepithelium (asterisk) and low to moderate levels in the spinal ganglia (arrows). Star, central canal. H, I: Bright and dark field photomicrographs of a transverse section through the cervical region showing high expression of the $T\beta_{10}$ gene in the mantle layer, which is pronounced in this region. Same symbols as in F and G. Scale bars: A, 500 μm; B–I, 200 μm.

mainly expressed in mesenchymal cells of most regions of the body such as mesenchymal condensations of the maxillar and mandibular processes, head mesenchyme surrounding the neural tube, sclerotome-derived mesenchyme of the trunk and the axis of the limb buds (Fig. 2A–C). The neural tube expresses very little $T\beta_{10}$ except in the scarce mantle layer found in the basal plate of the caudal medulla oblongata and rostral spinal cord (region of differentiating motoneurons), which shows a faint signal (Fig. 2B,C). A weak hybridization signal was also found in the rostral spinal ganglia. The cells of endocardial cushions showed a low to moderate signal. In the 10.5 dpc embryo, the pattern of $T\beta_{10}$ mRNA expression showed little variation compared to that observed in the 9.5 dpc stage. Changes were mainly detected in the neural tube where the expression is rather high in the mantle layer of the basal plate of the medulla and rostral spinal cord, and in the spinal ganglia of the corresponding segments (Fig. 2D,E). In the mesenchyme, the level of hybridization was similar to that observed in the previous stage (Fig. 2D,E) whereas the amount of $T\beta_{10}$ mRNA in the cells of endocardial cushions was slightly higher. At the 11.5 dpc stage, the $T\beta_{10}$ mRNA is located only in the mantle layer of the brain. This mantle layer is now clearly appreciable in the rostral spinal cord, medulla oblongata and midbrain. The thalamus shows in its thin mantle a moderate hybridization signal. The cranial (Gasserian, otic, etc.) and first spinal ganglia show a level of expression similar to that of the mantle layer. Expression in mesenchymal structures is similar to that observed in the for-

mer developmental stages. In the 12.5 dpc embryo, expression in the brain extends rostrally to the mantle layer which appeared in the striatum, thalamus and hypothalamus, but it cannot be distinguished in the telencephalic hemispheres (Fig. 2F,G). The mantle expressing $T\beta_{10}$ extends in the medulla oblongata laterally, including medial regions of the alar plate, although the hybridization is maximal near the midline. No expression of $T\beta_{10}$ mRNA is detected in the cerebellar lips where this layer is inappreciable. In the rostral spinal cord, this mantle layer has extended dorsally and the signal has increased correspondingly (Fig. 2F–I). The cranial and rostral spinal ganglia also present $T\beta_{10}$ mRNA but with an intensity lower than that found in the mantle layer. In caudal regions where the spinal cord only consists of neuroepithelium, no signals above the background levels were found. On the other hand, mesenchymal structures showed a high level of this transcript although chondroid masses showed a low level. Expression is rather high in the mesenchyme associated with the nephric ducts, the falciform process separating the liver from the thoracic cavity, and also it is appreciable in premuscular bands of limb buds and body wall. The amount of $T\beta_{10}$ mRNA is also high in the endocardial cushions but it is low or inappreciable in the cardiac muscle. Interestingly, $T\beta_{10}$ mRNA was absent in epiplexus cells (Kolmer cells) of the brain ventricles (Fig. 2, H–I) as well as in blood leukocytes (data not shown). The eye structures, the otocyst walls, nasal epithelia, Rathke's pouch, gut and kidney epithelia and the wall of blood vessels yielded a weak signal.

Comparison between the patterns of expression of $T\beta_4$ and $T\beta_{10}$ mRNAs in the early postimplantation mouse embryos shows interesting differences. We have reported that endothelial cells present in the wall of embryonic blood vessels contain large amounts of $T\beta_4$ mRNA [15]. Moreover, another group demonstrated that $T\beta_4$ antisense oligonucleotides blocked in vitro the formation of capillary-like tubes by the endothelial cells [19]. Both experiments implicate $T\beta_4$ in angiogenesis. In contrast, we have observed very low amounts of $T\beta_{10}$ mRNA in the wall of embryonic blood vessels (data not shown) suggesting that this peptide is not involved in angiogenesis. On the other hand, several types of migrating cells localized in different areas of the mouse embryo also produce high levels of $T\beta_4$ mRNA [13,15] but they do not express $T\beta_{10}$ mRNA, at least in significant concentrations. The expression of $T\beta_4$ and $T\beta_{10}$ during mouse neurodevelopment also shows remarkable differences. We detected low amounts of $T\beta_{10}$ mRNA in the peripheral ganglia, the structures of the nervous system with the highest levels of $T\beta_4$ [13]. The strongest $T\beta_{10}$ hybridization signal was localized in the mantle layer of spinal cord, a region where $T\beta_4$ is also abundant. In contrast, the neuroepithelium (ventricular layer) of the spinal cord had a faint expression of $T\beta_{10}$ mRNA whereas it expressed $T\beta_4$ at high levels.

Neuroepithelial cells are rapidly proliferating but they are not undergoing differentiation. In these cells changes in shape and position are taking place and therefore it is necessary an active cytoskeletal regulation. We have found that these cells express high levels of $T\beta_4$ [13] and low amounts of $T\beta_{10}$ (this work). In the neuroblasts that form the mantle layer the situation is different. These cells start to elaborate axonal and dendritic processes, undergo differentiation and migrate to specific locations. In these cells both β-thymosin genes are highly expressed ([13], and this paper). Moreover, the high expression of $T\beta_4$ but not of $T\beta_{10}$ in the peripheral ganglia suggests that these neurons, which are outgrowing processes instead of differentiating them, need $T\beta_4$ for the rapid growth of axons and dendrites. A possible explanation for these results is that $T\beta_4$ is needed to maintain an active cytoskeleton for highly dynamic actin-based movements such as the formation of axons and other cell processes, whereas $T\beta_{10}$ participates in actin-based functions required for differentiation. We have observed an important increase in the amount of $T\beta_4$ [13] and $T\beta_{10}$ (Fig. 1) between 6.5 to 7.5 dpc indicating that both thymosins are involved in the changes starting at this developmental stage, neurulation and the beginning of organogenesis. $T\beta_{10}$ is very abundant in the mammalian embryonic brain but it is virtually absent in the adult brain. In contrast, $T\beta_4$ levels only decline slightly following birth [7,9–11] suggesting that it participates in the neuritogenesis during postnatal life.

Acknowledgements: We are very grateful to Dr. A.K. Hall for providing us with the thymosin β_{10} probe and for his kindness. This work was supported by Xunta de Galicia (XUGA 20009B94). P.C. is the recipient of a predoctoral fellowship from Xunta de Galicia.

References

[1] Nachmias, V.T. (1993) Curr. Opin. Cell Biol. 5, 56–62.
[2] Safer, D. and Nachmias, V.T. (1994) BioEssays 16, 473–479.
[3] Hannappel, E., Xu, G., Morgan, J.I., Hempstead, J. and Horecker, B.L. (1982) Proc. Natl. Acad. Sci. USA 79, 2172–2175.
[4] Hannapel, E., Wartenberg, F. and Bustelo, X.R. (1989) Arch. Biochem. Biophys. 273, 396–402.
[5] Yu, F.-X., Lin, S.-C., Morrison-Bogorad, M., Atkinson, M.A. and Yin, H.L. (1993) J. Biol. Chem. 268, 502–509.
[6] Yu, F.X., Lin, S.-C., Morrison-Bogorad, M. and Yin, H.L. (1994) Cell Motil. Cytoskel. 27, 13–25.
[7] Lin, S.-C. and Morrison-Bogorad, M. (1990) J. Mol. Neurosci. 2, 35–44.
[8] Lugo, D.I., Chen, S.-C., Hall, A.K., Ziai, R., Hempstead, J.L. and Morgan, J.I. (1991) J. Neurochem. 56, 457–461.
[9] Condon, M.R. and Hall, A.K. (1992) J. Mol. Neurosci. 3, 165–170.
[10] Hall, A.K. (1991) Mol. Brain Res. 9, 175–177.
[11] Hall, A.K., Hempstead, J. and Morgan, J.I. (1990) Mol. Brain Res. 8, 129–135.
[12] Hall, A.K. (1992) J. Mol. Neurosci. 3, 155–163.
[13] Carpintero, P., Anadón, R., Franco del Amo, F. and Gómez-Márquez, J. (1995) Neurosci. Lett. 184, 63–66.
[14] Gómez-Márquez, J., Pedrares, J.I., Otero, A. and Anadón, R. (1993) Neurosci. Lett. 152, 41–44.
[15] Gómez-Márquez, J., Franco del Amo, F., Carpintero, P. and Anadón, R. (1996) Biochim. Biophys. Acta 1306, 187–193.
[16] McCarrick, J.W. and Andrews, P.W. (1992) in: Neuronal Cell Lines: A Practical Approach (Wood, J.N., Ed.), pp. 77–104. IRL Press, Oxford.
[17] Chomczynski, P. and Sacchi, N. (1987) Anal. Biochem. 162, 156–159.
[18] Martin, G.R., Wiley, L.M. and Damjanov, I. (1977) Dev. Biol. 61, 230–235.
[19] Grant, D.S., Kinsella, J.L., Kibbey, M.C., Laflamme, S., Burbelo, P.D., Goldstein, A.L. and Kleinman, H.K. (1995) J. Cell. Sci. 108, 3685–3694.